Phenotypic screening of the ReFRAME drug repurposing library to discover new drugs for treating sickle cell disease

Belhu Metaferia[a,1], Troy Cellmer[a,1], Emily B. Dunkelberger[a,1], Quan Li[a,1], Eric R. Henry[a,1], James Hofrichter[a], Dwayne Staton[b], Matthew M. Hsieh[c], Anna K. Conrey[d], John F. Tisdale[c], Arnab K. Chatterjee[e], Swee Lay Thein[d], and William A. Eaton[a,2]

Stem cell transplantation and genetic therapies offer potential cures for patients with sickle cell disease (SCD), but these options require advanced medical facilities and are expensive. Consequently, these treatments will not be available for many years to the majority of patients suffering from this disease. What is urgently needed now is an inexpensive oral drug in addition to hydroxyurea, the only drug approved by the FDA that inhibits sickle-hemoglobin polymerization. Here, we report the results of the first phase of our phenotypic screen of the 12,657 compounds of the Scripps ReFRAME drug repurposing library using a recently developed high-throughput assay to measure sickling times following deoxygenation to 0% oxygen of red cells from sickle trait individuals. The ReFRAME library is a very important collection because the compounds are either FDA-approved drugs or have been tested in clinical trials. From dose-response measurements, 106 of the 12,657 compounds exhibit statistically significant antisickling at concentrations ranging from 31 nM to 10 μM. Compounds that inhibit sickling of trait cells are also effective with SCD cells. As many as 21 of the 106 antisickling compounds emerge as potential drugs. This estimate is based on a comparison of inhibitory concentrations with free concentrations of oral drugs in human serum. Moreover, the expected therapeutic potential for each level of inhibition can be predicted from measurements of sickling times for cells from individuals with sickle syndromes of varying severity. Our results should motivate others to develop one or more of these 106 compounds into drugs for treating SCD.

sickle cell disease | antisickling drugs | hemoglobin S | phenotypic drug discovery | high-throughput drug screening

An abnormal hemoglobin (HbS) causes sickle cell disease (SCD), the first example of a "molecular disease" reported by the legendary chemist, Linus Pauling, in 1949 (1, 2). Pauling's discovery gave birth to the field of molecular medicine. This monogenic disease results from a single nucleotide change from A to T in the codon (GAG) of the gene for the Hb beta chain. The mutation results in the replacement of a negatively charged glutamate with a neutral, hydrophobic valine on the molecular surface, which creates a sticky patch that promotes polymerization of HbS upon deoxygenation to form fibers (3, 4). HbS polymerization in the tissues is the root cause of SCD pathology because the fibers stiffen and distort ("sickle") red cells. Sickled cells can cause vaso-occlusion in the smallest vessels of almost every tissue (5, 6), resulting in intermittent episodes of acute clinical events, the most prominent of which is pain that is so severe that it is commonly referred to as a sickle cell crisis (5, 6). In addition, the irreversible structural changes in the red cell cytoskeleton associated with sickling in the tissues and unsickling in the lungs cause red cell fragility and consequent hemolysis that underlies the chronic hemolytic anemia. The two hallmarks of recurrent vaso-occlusion and chronic hemolysis trigger and sustain a continuing background of inflammatory response leading to vasculopathy and acute and chronic damage to the brain, lungs, kidney, liver, and others. Inhibition of HbS polymerization is therefore the most rational drug treatment for the disease (7).

Hydroxyurea (HU), approved by the Food and Drug Administration (FDA) in 1998, is currently the only successful antisickling drug (8)[*], but its use is limited by its safety profile, which includes myelosuppression and thrombocytopenia. The efficacy of HU is due to its effect on various aspects of sickle pathophysiology; induction of fetal Hb (HbF), which inhibits HbS polymerization, is considered the most important. However,

Significance

The majority of patients suffering from sickle cell disease live in underresourced countries. Consequently, advanced medical facilities required for curative therapies, such as stem cell transplantation and gene therapy, will be unavailable to them for many years. Hydroxyurea, approved by the FDA in 1998, is the only effective drug that inhibits polymerization of the mutant hemoglobin S that stiffens and distorts ("sickles") red cells, the root cause of the pathology. What is urgently needed now for these patients are additional, inexpensive oral antisickling drugs. Our high-throughput phenotypic screen of the ReFRAME drug repurposing library reported here discovered 106 compounds that are antisickling. On a statistical concentration basis, as many as 21 are predicted to be potential drugs.

See online for related content such as Commentaries.

---

*The FDA has approved two other drugs: voxelotor and L-glutamine. Voxelotor inhibits sickling but does not reduce the frequency of sickle cell crises, which we have attributed to the decrease in oxygen delivery resulting from the left shift in the oxygen dissociation curve (9, 10). L-Glutamine apparently decreases the frequency of sickle cell crises by reducing oxidative stress, one of the sequelae of sickling (11). This drug is in the Calibr library, but did not survive our initial 10 μM screen (see below). We also recently repeated the experiment, which showed that L-glutamine does not inhibit sickling.

individual responses to HbF are variable based on clinical response and changes in hematological parameters (12, 13), and the increase in HbF is not evenly distributed in all cells (7, 14). Consequently, it is only partially effective (7, 14, 15). Thus, additional inexpensive oral drugs that inhibit sickling in all cells are urgently needed because the majority of patients in the world do not have, and for many years will not have, the necessary advanced medical facilities and resources required for curative therapies such as hematopoietic stem cell transplantation or gene therapy (16, 17). Now that large compound libraries are available, basic research scientists can engage in drug development using screening assays that are pathophysiologically relevant. We have recently developed a relevant high-throughput assay (18) to screen the Scripps California Institute of Biomedical Research (Calibr) ReFRAME drug repurposing library. This library is a unique and very important collection because the compounds are either FDA-approved drugs for other indications or have been tested in clinical trials with extensive drug annotation in an open-access format (reframedb.org) (19). Consequently, compounds that inhibit sickling at serum concentrations found in humans, without known side effects that would be deleterious to SCD patients, can be rapidly brought to clinical trial without extensive preclinical studies that markedly slow drug development. Since there is no specific molecular target, this approach is referred to as phenotypic drug discovery (20). In this work, we present the results so far from screening the 12,657 compounds of the Calibr library using our sickling assay (18).

Our previous screening assay used a 96-well plate format and laser photodissociation of carbon monoxide (CO) saturated sickle trait cells to rapidly create deoxyHbS in <1 s (21). The assay is extremely sensitive because it determines the delay time before sickle fiber formation for each cell, but it is low throughput and requires the use of sodium dithionite, a very strong reducing agent that could react with the test compound (9, 21). We were therefore motivated to develop a high-throughput assay under more physiological conditions without dithionite. Our current assay uses a 384-well plate format and is based on deoxygenation of sickle trait cells with nitrogen to 0% oxygen and acquisition of images of 100 to 300 cells in each well every 15 min using an Agilent "Lionheart" automated microscope system (18). With one instrument, up to ~1,300 compounds at a single concentration can be tested in 1 week, making our screen relatively high throughput; we now have four such instruments. As in the previous CO photolysis assay, the time at which individual cells change shape (sickle) is determined using automated image algorithms for characterizing red cell morphology, refined by machine learning (18).

There are many advantages to using cells from donors with sickle trait, the heterozygous condition (21). The delay time for polymerization is ~1,000-fold longer for trait cells than for SCD cells because of the much lower fraction of HbS in trait cells (35 to 40% HbS in trait cells compared to 85 to 95% in SCD cells) (22, 23). With longer delay times, there are many fewer primary nucleation events, resulting in only a few domains of fibers (24, 25). Consequently, cellular distortion is much greater (26), making the determination of sickling times more accurate. In addition, trait cells are less damaged and therefore are a much more homogeneous cell population than SCD cells (6, 27). There are many more trait blood donors, who very often have relatives with SCD and are therefore willing to donate as frequently as requested. While polymerization in trait cells is much slower, there is no evidence that the mechanism of sickle fiber formation is different (25). Nevertheless, it

is important that we demonstrate that inhibitors of trait cell sickling also inhibit the sickling of SCD cells.

There is every reason to expect that new drugs will be discovered from our screen because it tests for all but one of the five independent approaches that have been proposed to inhibit sickling as therapy (7). These four classes of inhibitory mechanisms, discussed in detail in reference 7, are (1) blocking intermolecular contacts in the sickle fiber; (2) destabilizing the fiber by decreasing 2,3-diphosphoglycerate (28, 29), with added destabilization resulting from the concomitant increase in intracellular pH (30–32); (3) decreasing the intracellular hemoglobin concentration, for example, by swelling red cells (21, 33); and (iv) preferentially shifting the R-T quaternary equilibrium toward the nonpolymerizing R conformation with a drug that both binds and dissociates very rapidly from the R quaternary conformation (9, 25, 34, 35). Since the assay measures the inhibition of mature cells in peripheral blood, it does not test for compounds that induce HbF synthesis in stem cells (14, 36–40). To assess this fifth independent approach, we make considerable use of the assay to measure the sickling of blood from individuals with SCD and sickle trait on various protocols and from patients who have been treated by using a virus to add globin genes to their stem cells for the nonpolymerizing HbF mimicking mutant, HbA(T87Q) (41).

Results

Images of Sickle Trait Cells upon Deoxygenation. Fig. 1 shows three typical images at 13 h after the start of deoxygenation: one for the negative control with 85% of cells sickled, one for the positive control with no cells sickled, and one for a test compound that shows 40% of cells sickled. To have a sufficient number of cells in each image at acceptable resolution for the automated image analysis, a 20× objective with a numerical aperture of 0.45 was used. Consequently, the resolution of the images is suboptimal. Nevertheless, the cellular distortions are more than sufficient to determine at each time point whether a cell is sufficiently distorted to label it as sickled. The three most obvious changes are the loss of a circularity, the loss of a more transparent center because of the loss of concavity in the middle of the cell, and the decrease in the projected area of the cell. The time at which a cell sickles is determined by a change in at least two of these metrics compared to the previous time point. The output of the analysis is the fraction of cells sickled as a function of time. The *SI Appendix* contains a video of images following the start of deoxygenation.

Fraction Sickled versus Time and Dose-Response Results. Fig. 2*A* shows the time courses for different concentrations of the test compound calcimycin, as well as for the negative and positive controls of the fraction sickled following the start of deoxygenation to 0% oxygen with nitrogen to induce HbS polymerization and sickling. Also shown with these sickling curves are the singular value decomposition (SVD) of the curves and the dose-response results (Fig. 2*B*), which showed 50% inhibition (IC$_{50}$) at a concentration of 2.1 ± 0.1 μM. SVD is a powerful matrix-analytic method for averaging data to eliminate noise and provides the best least-squares representation of the results with smooth curves that simplifies the quantitative analysis of massive datasets (42). SVD of the measured sickling curves is described in detail in the *Materials and Methods* section. The three colors correspond to the results for red cells from three different sickle trait donors. This set of experiments is not representative but shows how good the data can be when almost every aspect of the experiment and image analysis works nearly perfectly. In this case the differences among the donor samples for the negative controls are
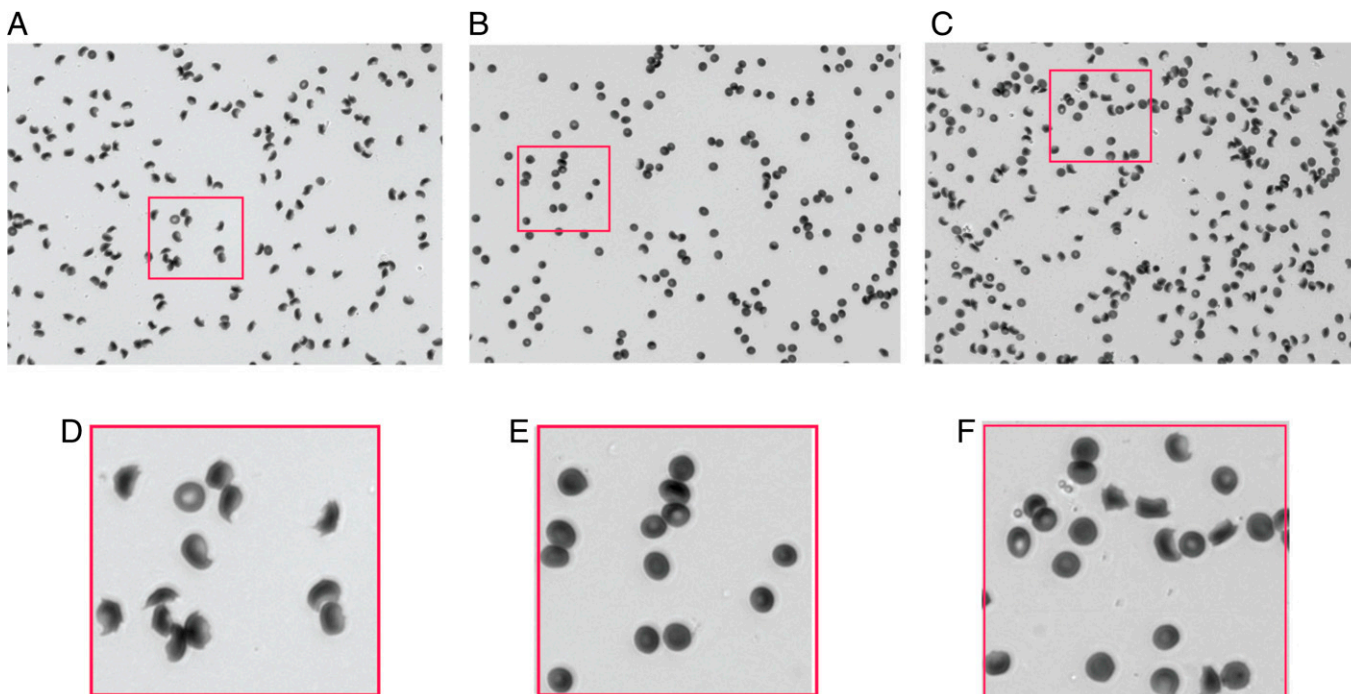
Fig. 1. Images of sickle trait cells. (*A*) Negative control at end of experiment (13 h after start of deoxygenation). (*B*) Positive control at end of experiment (13 h after start of deoxygenation). (*C*) Well containing 10 µM of phanquinone (13 h after start of deoxygenation). The fraction sickled in the negative control for this well is 0.85, while the fraction in the well containing phanquinone is 0.40. There are 172, 175, and 236 cells in each of these images, respectively. (*D–F*) Enlarged sections of images in panels (*A*)–(*C*), respectively.

much larger than usual because of large differences in Hb composition and intracellular Hb concentration (MCHC, the clinical laboratory term, mean corpuscular hemoglobin concentration), which are the two most important factors that determine the rate and extent of sickling. Cells from donor 1 sickle the most because they contain the largest percentage of HbS and the highest MCHC. Nevertheless, the fraction sickled as a function of compound concentrations relative to the negative control is very similar for cells from all three donors (Fig. 2*B*).

Fig. 3 is more representative of the results for all of the compounds measured. Four additional representative datasets are provided in the *SI Appendix*. All of the dose-response plots, as in Figs. 2*B* and 3*B*, for an additional 97 of the 106 compounds found to be antisickling are given in the *SI Appendix*.

Table 1 summarizes our main results. It gives the compound name, the concentration that produces 50% inhibition (IC_{50}), and the lowest concentration that produces statistically significant inhibition (LIC), defined by $(\langle V1_{nc}\rangle - V1_{cpd})/\sigma_{nc} > 3$, where $\langle V1_{nc}\rangle$ is the average value of the amplitude (V1) of U1 for the sickling curves of the negative controls (nc), $V1_{cpd}$ is the amplitude of U1 for the sickling curve of the test compound, and σ_{nc} is the SD of $\langle V1_{nc}\rangle$. See *Materials and Methods* for a description of the U1s and V1s, the first components of the **U** and **V** matrices of the SVD.

Comparing Sickling Inhibition of Sickle Trait and SCD Cells. To determine whether compounds that inhibit sickling of cells from sickle trait donors also inhibit sickling of cells from SCD patients, a comparison was carried out for several of the antisickling compounds discovered in the screen. Compounds for these experiments were purchased from commercial sources (see company names in *Materials and Methods*). To have roughly comparable sickling curves for the negative controls of both SCD and trait cells, SCD cells were deoxygenated to 5% oxygen to slow polymerization; trait cells were deoxygenated to

0% oxygen as in the screen. Fig. 4 shows a comparison of the sickling curves for trait and SCD cells for 14 of the antisickling compounds in Table 1 and *SI Appendix*, Table S1.

Comparing Antisickling Concentrations with Serum Concentrations of Oral Drugs in the *Physician's Desk Reference* (*PDR*). The distribution of maximum free concentrations (C_{max}) for oral drugs in the *PDR* is shown in Fig. 5*A*. The free C_{max} is the maximum free concentration of a drug for the given dosage regimen. Fig. 5*B* shows the number of antisickling compounds at each concentration for which there is statistically significant inhibition of sickling, as well as the probable number in parentheses that would be expected to be oral drugs based solely on the concentration distribution in Fig. 5*A*. From this analysis, there are as many as 21 potential drugs for treating SCD.

Sickling Curves for Sickle Syndromes. To assess the therapeutic potential for a given level of sickling inhibition, we compared the sickling curves for red cells from donors with various sickle syndromes. Fig. 6*A* shows the average sickling curves from deoxygenation to 5% oxygen for red cells from 65 HbSS SCD patients being treated with HU, 31 HbSS SCD patients not taking HU, 9 HbSC disease patients not taking HU, 9 HbSS SCD patients after HbA(T87Q) globin addition gene therapy (43, 44), an individual who is a compound heterozygote for HbS and pancellular distribution of hereditary persistence of HbF (HbS/HPFH), and from 9 individuals with sickle trait (AS). Fig. 6*B* shows the area under the sickling curve (AUSC) for each condition (in the SVD analysis, the area under V1xS1xU1 is an accurate approximation to the AUSC). The SDs in Fig. 6*B* result from person-to-person differences, primarily due to differences in Hb composition and MCHC, with little or no contribution from experimental error. The HbS/HPFH individual and the 9 HbSS SCD patients treated with HbA(T87Q) gene addition therapy were asymptomatic at the time of the sickling measurements.
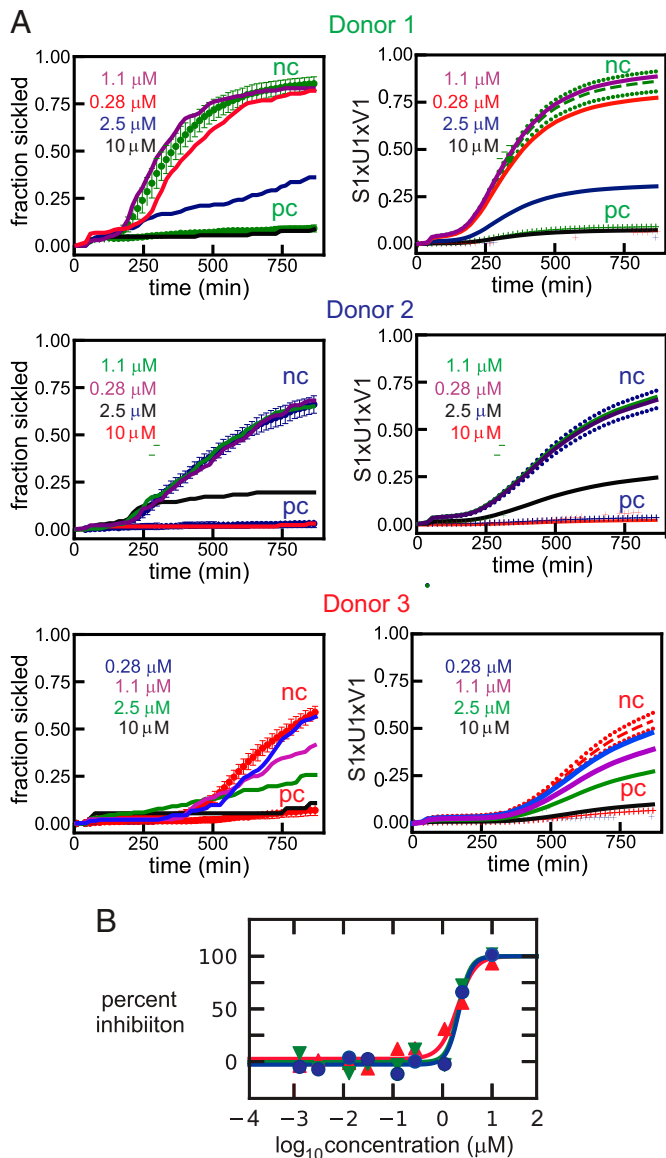
Fig. 2. Nonrepresentative dose-response data for ReFRAME compound calcimycin, an antibiotic. (*A*) Time course of the fraction sickled following the start of deoxygenation with nitrogen to induce HbS polymerization and sickling. Sickling curves are shown at four different concentrations of calcimycin. Panels on the left are the measured sickling curves, while panels on the right show the curves constructed using only the first component of the SVD. The continuous curves in both left and right panels are the sickling curves for the single wells containing the test compound. The three colors represent samples from three different sickle trait donors with Hb compositions as percentage of total Hb: donor 1: HbA 56.0, HbS 38.0, HbA2 4.0, HbF 1.2, MCHC 34.2 g/dL; donor 2: HbA 62.7, HbS 33.7, HbA2 3.5, HbF <1.0, MCHC 28.6 g/dL; donor 3: HbA 59.7, HbS 37.8, HbA2 3.8, HbF <1.0, MCHC 26.6 g/dL. In the left panels, the upper points are the average for 12 negative controls (no compound) and SDs from the average, while the lower points are the average for 6 positive controls (osmotically swollen cells) and SDs from the average. In the right panels, the dashed curves are the average sickling curves (S1 × U1 × V1) of the negative controls with SDs indicated by the dotted curves. The lower points and vertical bars are the average and SDs for the positive controls. The abbreviations nc and pc stand for negative control and positive control, respectively. (*B*) Points are measured percentage of inhibition defined by Eq. 1 for cells from 3 different donors, while the continuous curves are the fits to the data using Eq. 2 (see *Materials and Methods* section for equations).

Discussion

The assay used in this screen must be considered quite relevant to the pathophysiology of SCD since HbS polymerization and consequent red cell sickling is the root cause of the pathology.

Even though sickling in this assay is occurring on the tens of minutes to hours timescale, it remains relevant to sickling on the in vivo timescale of seconds. The reason is that the delay time for polymerization and sickling has been shown to depend on the supersaturation (the ratio of the total Hb concentration in the cell to the solubility) at all timescales from milliseconds to 1 day (57).

The assay is also relatively high-throughput, as evidenced by the fact that ~80,000 sickling curves were measured in the screen, each one consisting of evaluating images of red cells at 50 time points for 100 to 300 cells in each well of 210 plates containing 384 wells for a total of >400 million red cell images. The screen was carried out in two stages. In the first stage, sickling curves were measured in triplicate for all 12,657 compounds at a concentration of 10 μM, which were incubated
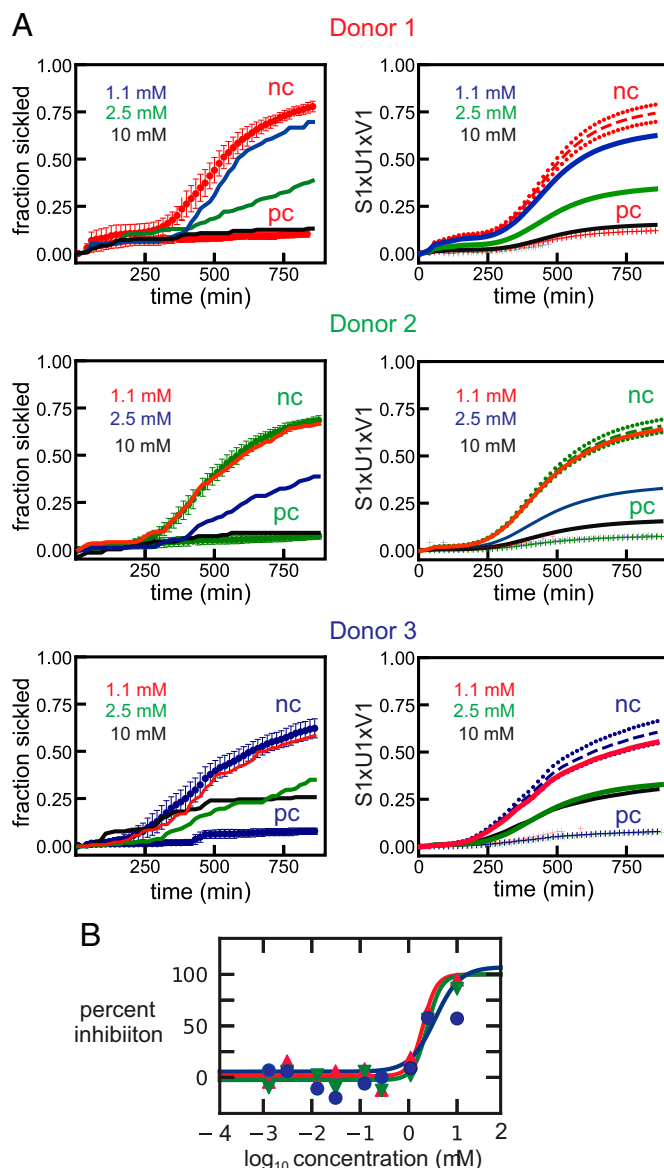

Fig. 3. (*A*) More representative dose-response data for ReFRAME compound NSC-150117, a phosphatase inhibitor. The legend is the same as in Fig. 2, except for the hemoglobin compositions as percentage of total Hb of the donors , which are: donor 1: HbA 56.1, HbS 40.0, HbA2 3.7, HbF <1.0, MCHC 29.8 g/dL; donor 2: HbA 59.8, HbS 35.5, HbA2 3.8, HbF <1.0, MCHC 33.6 g/dL; donor 3: HbA 59.7, HbS 37.8, HbA2 3.8, HbF <1.0, MCHC 26.6 g/dL. (*B*) Points are measured percentage of inhibition defined by Eq. 1 for cells from 3 different donors, while the continuous curves are the fits to the data using Eq. 2 (see Materials and Methods section for equations).

Table 1. List of antisickling compounds with LICs <10 μM

Name of compound	IC50 (μM)[*]	LIC (μM)[†]
Ammonium trichlorotellurate[‡,§]	0.032 ± 0.015	0.031
Niferidil[‡,**]	10.5	0.031
Mavatrep	0.23 ± 0.14	0.123
Manoalide[‡]	0.33 ± 0.09	0.278
HR325[‡]	3.0 ± 0.86	0.278
NSD-721[‡]	13 ± 2.0	0.278
FT-11[‡]	1.3 ± 1.0	0.278
Mitapivat[‡]	0.25 ± 0.16	0.278
ARA DMAP[‡]	3.9 ± 1.1	1.1
Pafuramidine[‡]	6.0 ± 5.8	1.1
Cisplatin[‡,§,¶]	1.3 ± 0.2	1.1
Cloturin[‡,‖]	9.7 ± 0.5	1.1
EF-4040[‡]	1.7 ± 0.4	1.1
Cyclovalone[‡]	1.7 ± 0.7	1.1
VML 530	1.5 ± 0.2	1.1
Peruvoside[‡]	NA[#]	1.1
ONO-7746	3.8 ± 2.0	1.1
BMS-919373[§,¶,‖]	6.4 ± 8.1	1.1
KUX-1151[‡]	5.3 ± 5.1	1.1
NT-113	3.6 ± 2.8	1.1
Curcumin	0.50 ± 0.14	1.1
AEG-33783[‡,§]	1.4 ± 0.5	1.1
VRT-532[‡]	5.8 ± 0.7	2.5
Licochalcone A	4.3 ± 2.4	2.5
NSC-150117	2.6 ± 0.7	2.5
AT-101[§]	2.4 ± 0.1	2.5
Darapladib[§,¶]	2.0 ± 0.4	2.5
Oxyfedrine hydrochloride	2.9 ± 1.1	2.5
Octenidine[‡,§,¶]	NA[#]	2.5
WP-1066[‡]	3.9 ± 1.2	2.5
Butein	10 ± 3	2.5
Ethacrynic acid[‡]	3.3 ± 0.9	2.5
TS-80[‡]	3.1 ± 1.6	2.5
SC-1	10 ± 5	2.5
Tucaresol	3.1 ± 0.3	2.5
CBS-1114	7.2 ± 5.2	2.5
YM 57158	2.5 ± 0.3	2.5
Allisartan[‡]	7.8 ± 4.6	2.5
Elisartan potassium	5.6 ± 4.0	2.5
Samixogrel	4.2 ± 2.0	2.5
AM-103[‡,§,‖]	4.5 ± 2.6	2.5
ODM-103[‡,‖]	9.0 ± 2.2	2.5
ON-09310	5.9 ± 1.7	2.5
P-7435[‡]	NA[#]	2.5
AZD-4769	2.5 ± 0.9	2.5
Calcimycin	2.1 ± 0.1	2.5
Vadadustat[‡]	7.9 ± 6.3	2.5
Metabromsalan[‡]	8.0 ± 2.5	2.5
IMD-0560	2.3 ± 1.1	2.5
Laflunimus	7.2 ± 3.7	2.5

NA, not applicable.
[*]Concentration that produces 50% inhibition.
[†]Lowest concentration of statistically significant inhibition.
[‡]LIC is antisickling for cells from two of three donors.
[§]Compound causes lysis at high concentration, antisickling at lower concentration.
[¶]Incubated for 8 h.
[#]IC50s could not be determined for these three compounds because of an insufficient number of data points higher than 0% inhibition.
[‖]IC50s could only be determined for two of the three donor samples for these compounds because of an insufficient number of data points higher than 0% inhibition.
[**]IC50s could only be determined for one of the donor samples for these compounds because of an insufficient number of data points higher than 0% inhibition.

for 3 h before the start of deoxygenation. In the second stage, dose-response measurements were made at concentrations ranging from 1 nM to 10 μM for red cells from three different sickle trait donors for compounds that were judged to be antisickling from the first stage. Since we had previously shown in our sickling study of the ionophores monensin and gramicidin that compounds can increase cell volume extremely slowly (21), we list in *SI Appendix*, Table S2, 20 compounds that caused lysis at 10 μM, but did not inhibit at a lower concentration. These compounds should be reinvestigated in the future with 24-h incubations. For the lowest inhibitory concentration of the 106 compounds listed in Table 1 and *SI Appendix*, Table S1, 59 inhibited sickling of cells from all 3 trait donors, while 47 inhibited sickling of cells from 2 of 3 donors. As is common in research, because of failed experiments and flaws in our first analysis of the massive amount of data, the course of the experiments did not follow the original plan but took a somewhat tortuous path to finalizing the number of antisickling compounds. The detailed path is provided in the *SI Appendix*.

A critical factor for assessing therapeutic potential is to compare concentrations of antisickling compounds in our assay with serum concentrations in humans. To obtain an estimate of how many of the 106 antisickling compounds in Table 1 and *SI Appendix*, Table S1, are expected to be potential drugs based on their inhibitory concentration (Fig. 5*B*), we searched the *PDR* for the free concentrations (i.e., not bound to serum proteins) of oral drugs (Fig. 5*A*). Assuming that the distribution of free serum concentrations of the 106 antisickling compounds discovered in our screen is the same as the distribution in the *PDR*, this analysis suggests that as many as 21 compounds inhibit sickling at concentrations similar to or lower than the free concentrations observed in the plasma following oral administration. These agents therefore offer potential for the treatment of SCD (Fig. 5*B*). There are obvious caveats to using only free serum concentrations for predicting potential drugs. A drug for SCD must be taken for the lifetime of the patient and side effects that are tolerable for patients with other diseases may not be tolerable for sickle cell patients. Compounds may also be metabolized to a form that is less or even not antisickling, or have unfavorable pharmacokinetic properties.

For the multiple reasons described in the introduction, our screen was carried out using cells from donors with sickle trait. It was therefore important to show that compounds, which inhibit sickling of trait cells, also inhibit sickling of SCD cells. Negative controls for trait cells deoxygenated to 0% oxygen and SCD cells deoxygenated to 5% oxygen to slow sickling rarely have the same amplitude and shape, so it is difficult to make a perfect comparison of inhibitory effects of a test compound for the two cell types. Nevertheless, comparing sickling curves for samples from SCD and trait individuals in Fig. 4 strongly supports the conclusion that inhibition is very similar. We may have expected larger differences than those observed in Fig. 4, since SCD cells are more damaged than trait cells from the much more frequent sickling/unsickling cycles in vivo. The fact that they are so similar has important implications for clinical trials, for it indicates that measurements of sickling for sickle trait patients as healthy volunteers in Phase I clinical trials for a potential antisickling drug should be predictive of the results for Phase II trials for SCD patients.

To make a rough assessment of the expected therapeutic potential for a given level of sickling inhibition, we compared the sickling curves for several sickle syndromes in which the final oxygen concentration was 5% (Fig. 6). Given that no
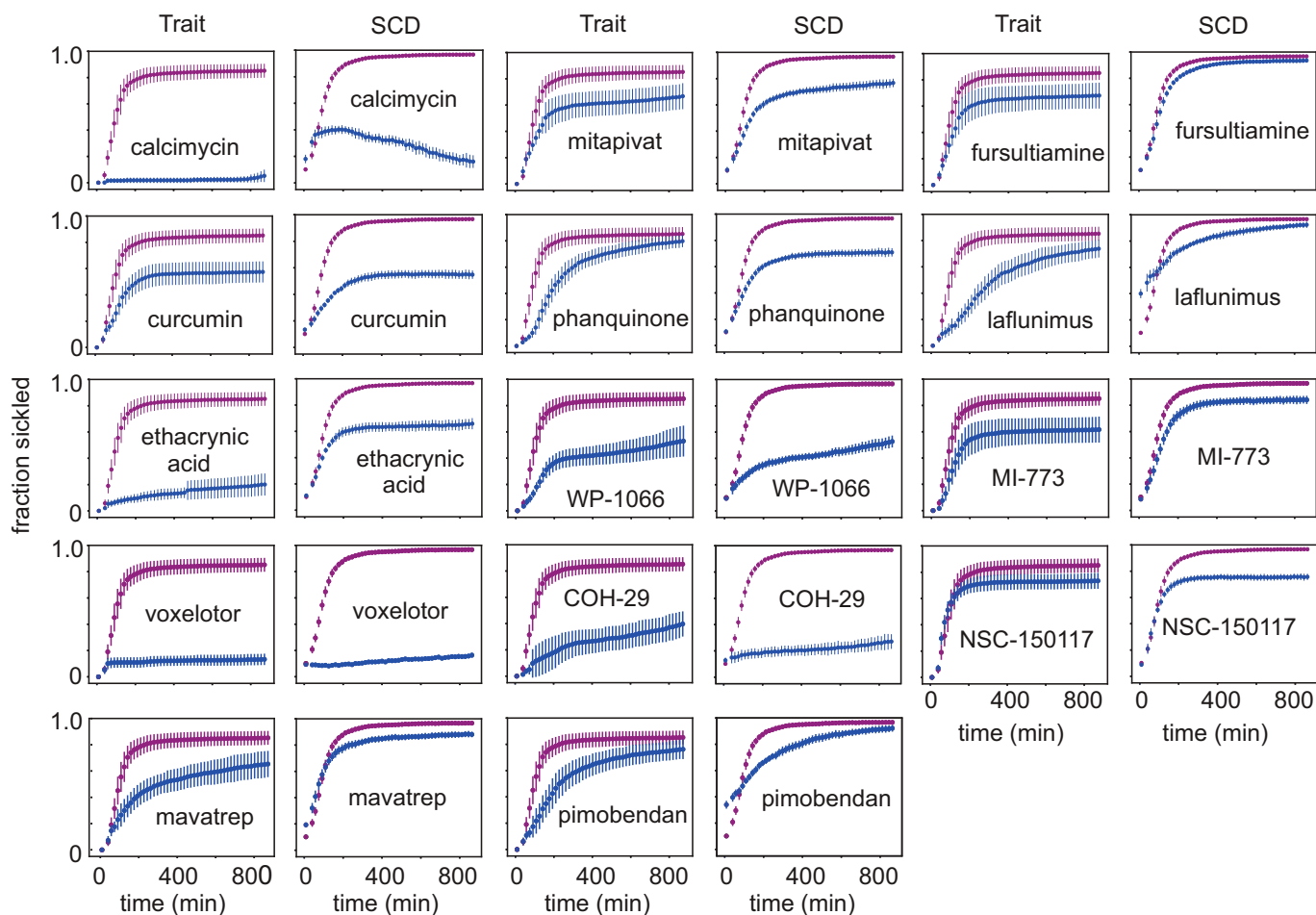
Fig. 4. Comparing antisickling compounds in sickle trait and SCD cells. Fraction sickled versus time following deoxygenation to 0% oxygen for cells from sickle trait individual (HbA 56.1%, HbS 40%, HbA2 3.7%, HbF <1.0%, MCHC 29.5 g/dL) and deoxygenation to 5% oxygen for cells from SCD patient (HbS 91%, HbA2 4.2%, HbF 4.8%, MCHC 34.8 g/dL) incubated for 3 h at a concentration of 10 μM for 14 of the 106 antisickling compounds listed in Table 1. In all of the plots, the x axis runs from 0 to 900 min, and the y axis runs from 0 to 1, both with slight offsets from 0. The upper curves (purple) are negative controls; lower curves (blue) are for test compounds. The SDs are larger for trait cells because the average number of cells in the images was approximately twofold less than for SCD cells. The unusual sickling curve for SCD cells incubated with calcimycin suggests that fibers, which form, subsequently melt as the effect of the drug is increasing, presumably because of a volume increase large enough to result in an intracellular concentration less than the solubility.

sickling is found for sickle trait cells with deoxygenation to 5% oxygen, the surprise was the observation of considerable sickling for cells from an asymptomatic individual with HbS/HPFH and for cells from SCD patients effectively cured by HbA(T87Q) gene addition therapy (41) (Q in position 87 of the γ chain of HbF is believed to be primarily responsible for reducing the copolymerization of tetramers containing γ chains (45)). There is much more sickling of HbSC cells than of trait cells even though HbS is usually only ~10% higher than in trait cells. This has been previously explained by an increased intracellular HbS concentration in SCD (46, 47). In our HbSC patients, the average concentration is ~5 to 7% higher than in trait cells (see Table 2 and ref. (48)), which decreases the delay time 4- to 8-fold ($\sim 1.05^{30}$ and $\sim 1.07^{30}$) to produce more sickling than for trait cells (7, 25, 30, 49–52). Comparing sickling curves in Fig. 6 leads to the intriguing suggestion that there is a narrow range of sickling that divides asymptomatic and symptomatic individuals.

The positive news for drug development from the results in Fig. 6 is that even a small reduction in sickling will be therapeutic, as observed for cells from SCD patients being treated with HU. Moreover, the results for HbS/HPFH and HbA(T87Q) cells predict a major (even "curative") therapeutic effect if serum concentrations that reduce sickling twofold

(the IC_{50}s in Table 1 and *SI Appendix*, Table S1) could be achieved.

Because they lyse cells but inhibit sickling at lower concentrations, we already know 17 compounds (indicated in Table 1 and *SI Appendix*, Table S1, footnote[§]) that belong to the class of antisickling mechanisms that increase cell volume to decrease the intracellular HbS concentration. The concept of decreasing the intracellular HbS concentration followed immediately on the decades-old observation that the delay time before detectable fiber formation depends on a very high power of the HbS concentration—the 30th power in the initial experiments (49)—which remains the highest concentration dependence ever observed for any molecular process. It also motivated approaches to treat the disease by decreasing the intracellular HbS concentration by means other than by increasing red cell volume (21, 53), such as introducing an iron-deficiency anemia. There are multiple way of making cells iron deficient,

---

[§]Mitapivat, one of the agents that demonstrated potential antisickling properties in the screen (Table 1), has been tested in a Phase I study in patients with SCD (56). Mitapivat is an activator of red cell pyruvate kinase (PKR). The study established proof of concept that activating PKR is a viable therapeutic approach for SCD, it improved hematologic parameters, increased oxygen affinity, and reduced sickling in patients with SCD. Results from this study informed the design of an ongoing Phase II/III trial of mitapivat in patients with SCD (RISE UP; NCT05031780), evaluating both improvements in Hb and frequency of sickle cell pain crises.
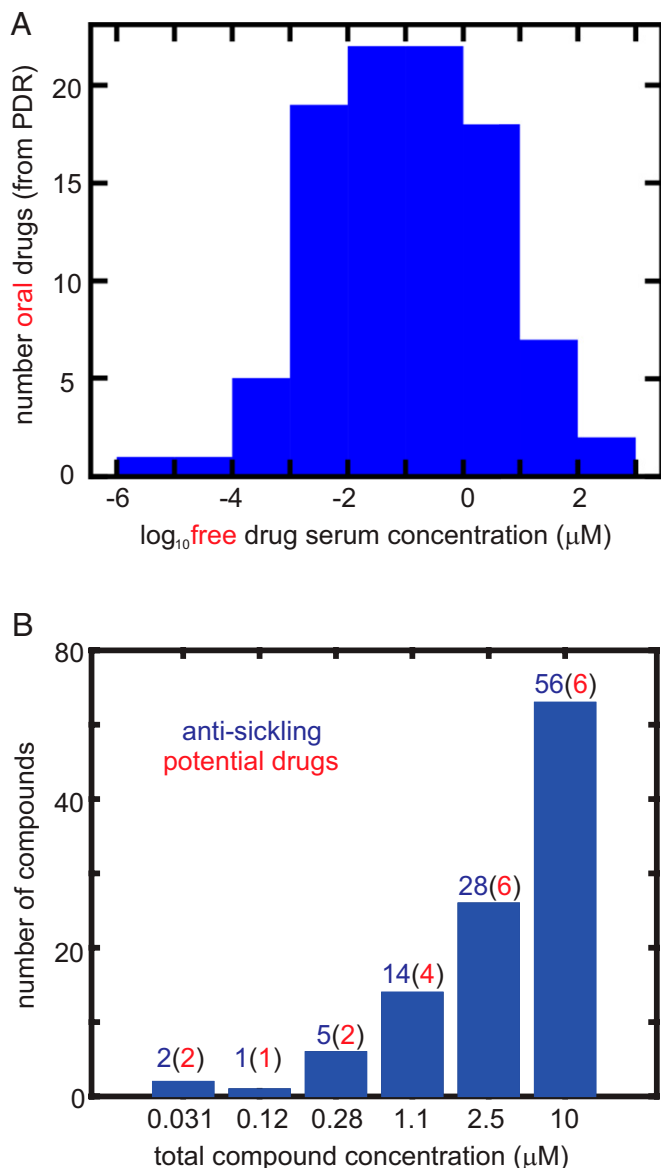
Fig. 5. Comparing inhibitory concentrations in assay and oral drug concentrations in the *PDR*. (*A*) Distribution of 97 free oral drug concentrations (C_{max}) in the 2015 version of the *PDR*. The free concentration was given either explicitly in the *PDR* or was obtained from the given total serum C_{max} and the percentage bound to serum proteins. (*B*) Distribution of ReFRAME total compound concentrations with statistically significant inhibition at each concentration, defined as $(\langle V1_{nc}\rangle - V1_{cpd})/\sigma_{nc} > 3$. The red numbers in parentheses result from multiplying the number (in blue) of compounds by the fraction of oral drugs with that free concentration or higher from the distribution in Fig. 5*A*. In the 2,000-fold diluted blood used for the assay, the Hb molecule is at a concentration of ~1 μM, while the molar concentration of red cells is ~4 fmol. Consequently, for inhibitory mechanisms other than those resulting from binding to Hb, the total compound concentration in the assay is also the free concentration. For compounds that inhibit by binding to Hb, the free concentration is less than the total concentration.

including restricting iron, using chelating agents, inhibiting the enzymes that catalyze heme synthesis, and even using what may be regarded as the heretical method of phlebotomy (7, 33, 54), the method used by physicians to treat illnesses 2,000 y ago, most notably by the Greek Hippocrates and the Roman Galen, who subscribed to the theory that disease was caused by too much blood, one of the four "humors."

Our next step is determine the mechanism of inhibition for each of the 106 antisickling compounds to determine which ones could be administered together as noncompetitive

inhibitors because they have different targets.[†] To accurately determine the detailed inhibitory mechanisms and the partitioning of the 106 compounds between serum and red cells for comparing inhibitory concentrations in vitro with achievable serum concentrations in vivo will require many person-years of research. It therefore seems important to publish all of the results we have so far, which should motivate others to develop one or more of the 106 antisickling compounds discovered in this study into urgently needed, inexpensive drugs for treating SCD.[‡,§] Although our primary goal is to discover an inexpensive pill, we should also consider the possibility that some of these compounds could be administered intravenously to abort or ameliorate a sickle cell crisis.

Materials and Methods

Sickling Assay. Blood samples were collected in ethylenediaminetetraacetate from anonymized donors with sickle trait according to NIH protocol 08-DK-0004 approved by the National Institute of Diabetes and Digestive Diseases institutional review board. Blood samples from patients with SCD (SCD-HbSS, HbSC and HbS/HPFH) in steady-state were collected in accordance with protocol 18-H-0146/NCT03685721 or 03-H-015/NCT00047996 or SCD patients treated by HbA(T87Q) global addition therapy in accordance with protocols 14-H-0155 and 20-H-0141; these protocols were approved by the National Heart, Lung, and Blood Institute institutional review board. The blood from sickle trait donors was diluted 2,000-fold into a phosphate-buffered saline (PBS) solution, while the blood from SCD patients was diluted 1,000-fold. The PBS consisted of 20 mM sodium/potassium phosphate, 155 mM sodium chloride, 300 mOsm, pH 7.4, 1 mg/mL dextrose, and no albumin or other protein. A total of 10 μL of these cell suspensions in every well resulted in 100 to 300 cells in the image at the bottom of the wells of a polypropylene Corning 384-well plate (part no. 3770, Corning, Corning, NY). To improve mixing with the test compound, the plates were shaken on the Compact Digital Microplate Shaker (Thermo Scientific, Waltham, MA) for 1 min. The well plate was then inserted into the humidified chamber at 37 °C of an Agilent Lionheart FX Automated Microscope (Agilent Technologies, Santa Clara, CA). A band-pass filter (Thorlabs [Newton, NJ], full width at half-maximum = 10 ± 2 nm) at 430 nm, the peak of the deoxyHbS absorption spectrum, was added to the light path of the instrument for filtering the white light source to improve image contrast. The flow of nitrogen from the building liquid nitrogen source into the chamber containing the well plate was controlled by the Agilent gas controller (part no. 1210013). Zero percent nitrogen for trait cells or 5% oxygen for SCD cells inside the chamber was reached in 20 to 30 min. At 5% oxygen, sickling of SCD cells is sufficiently slowed because of the decreased supersaturation (57) that deoxygenation is not rate limiting for sickling. Before preparing the well plate containing SCD cells, the blood was exposed to 100% oxygen at ice temperature to melt any residual polymer that would eliminate

---

[†]Calibr provided the compounds required for screening as spotted well plates, with each well containing <100 ng. For mechanistic studies, we will acquire milligram quantities of all 106 antisickling compounds. The class of mechanism to which a particular compound belongs will be determined from measurements of cell volumes for assessing changes in intracellular HbS concentration, measurement of oxygen dissociation curves to detect preferential binding to the R quaternary conformation, and application of our laser CO photolysis assay (21) or the Wood-Sachs FRET and dynamic light scattering methods (55) on dilute HbS solutions to detect destabilization of the fiber.

[‡]After this work was completed, we became aware of another high-throughput and extremely interesting assay based on detecting prenuclear oligomers in dilute solutions of purified HbS using fluorescence by Wood et al. (55). In a screen of the LOPAC[1280] compound library they discovered three antipolymerization compounds that do not alter oxygen affinity: chlormezanone, gabazine, and phosphoramidon disodium. At 500 μM concentrations, these compounds also inhibit polymerization inside red cells as judged by a microfluidic rheological assay of whole blood at a hematocrit of 25%, a typical value in SCD. In the dilute solution assay, however, 100 μM of these compounds were required to observe inhibition, whereas only ~2% of oral drugs are found in human serum at free concentrations of ≥100 μM. Moreover, chlormezanone was one of the compounds in the Calibr-Scripps library and showed no inhibition at 10 μM. With the current information it seems unlikely that any of the three compounds could be developed into oral drugs for SCD. We should emphasize, however, that the demonstration of inhibition of prenuclear aggregation inhibiting intracellular HbS polymerization is a very important finding. In our future work on determining the mechanism of sickling inhibition of our 106 hit compounds, we will use the very important dynamic light scattering and FRET assays of Wood et al. to determine which ones act by blocking intermolecular contacts in the sickle fiber. Fortunately, we can use our Agilent Lionheart automated microscope system for these experiments because it was actually designed for fluorescence measurements.
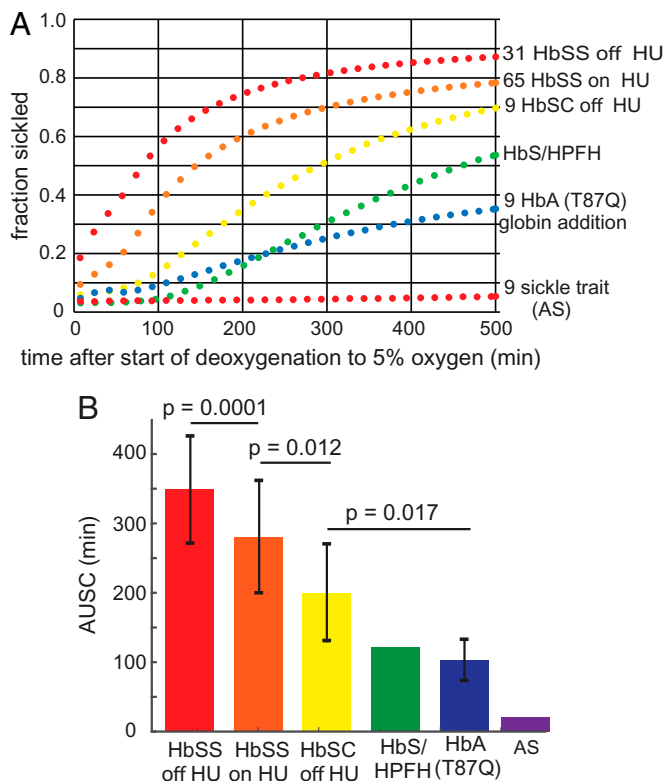
Fig. 6. Average sickling curves for red cells from individuals with various sickle syndromes. (*A*) Sickling curves: the condition and number of samples are given next to each curve. The average compositions and MCHCs and SDs from the average for each condition are given in Table 2. (*B*) Histogram of average AUSCs, SDs, and the statistical significance probability (*P* values) using an unpaired, two-tailed *t* test with the program Prism. The SDs are almost entirely due to person-to-person difference, with very little contribution from experimental error.

the delay period (58). After a 3-h incubation period to allow for the test compound to bind to its target, deoxygenation was started and continued for 10 to 12 h with images of cells collected every 15 min.

For the initial screen of all 12,657 compounds, wells were spotted by Calibr with 100 pmol of each compound for a concentration of 10 μM after the addition of 10 μL of the dilute red cell suspension. For dose-response measurements, the wells contained from 10 fmol to 100 pmol spaced at approximately factors of three intervals to give compound concentrations from ~1 nM to 10 μM. Triplicate plates for both the initial screen and dose-response measurements were provided by Calibr to assess differences in the inhibitory response for trait cells from three different donors. Cells containing no test compound in the wells of two columns of the plate served as negative controls; cells in wells of two columns in 170 mOsm PBS and containing no test compound served as positive controls. The hypo-osmotic effect of 170 mOsm swells cells and often so much so that the cells are sphered, which increases the cell volume by a factor of ~1.4 (59). Swelling reduces the intracellular hemoglobin concentration sufficiently to completely prevent sickling for ≥12 h because of the enormous sensitivity of the polymerization kinetics to the Hb concentration (the 30th power concentration dependence results in a 30,000-fold increase in the delay time for a 1.4-fold decrease in concentration (25)).

In comparing sickling for sickle trait and SCD cells in Fig. 4, all 14 compounds were purchased. The sources were curcumin (Sigma, St. Louis, MO), voxelotor (MedChem, Lexington, MA), mavatrep (MedChem), entrectinib (MedChem), pimobedan (MedChem), calcimycin (Medchem), laflunimus (MedChem), MI-773 (MedChem), COH-29 (Medchem), fursultiamine (MedChem), WP-1066 (MedChem), NSC-150117 (MedChem), etacrynic acid (Sigma), phanquinone (Sigma), and mitapivat (SelleckChem, Houston, TX).

Image Analysis. The image analysis is based on the fact that fiber formation is the only possible cause of a change in red cell morphology at optical microscope resolution, apart from rare fluctuations that tilt red cells onto an edge that gives an elongated projection counted as sickled. This is strongly supported by the observation in single SCD cells that changes in cell morphology and scattered light caused by polymerization are simultaneous (58) and the images of cell morphology shown to contain polymerized HbS from measurements of oxygen binding for individual cells (60, 61). The most important metrics for detecting a morphologic change are the loss of roundness, the loss of a more transparent center, and the decrease in the projected area of the cell. Two kinds of analysis were performed. In one, the sickling time was determined as the time when at least two of the three metrics of the cell image changed in the appropriate direction compared to the preceding image ~15 min earlier. In the second, machine learning was used, in which a model was constructed from the assignment by an experienced observer of ~1,000 cells as either sickled or not sickled based on the above three metrics (see ref. 5 for more details). Machine learning is particularly useful for analyzing images of SCD cells, since cells in the very first image, when there is no deoxygenation, so-called irreversibly sickle cells (ISCs), are counted as sickled, while in the first analysis they would not be counted because the shape of ISCs may not change at all when fibers form during the 10- to 12-h course of the experiment. The output of an experiment is a plot of the fraction sickled versus time for cells incubated with each library compound and the average fraction sickled versus time and SD from the average fraction at each time point for the negative and positive controls.

SVD of Sickling Curves. For analysis of the sickling curves, the powerful matrix-analytic method of SVD of the data was used (42). The data consist of the fraction sickled at 50 time points following the start of deoxygenation. The data matrix, **D** is a 50 × 384 matrix. SVD exactly reproduces **D**, including the noise, with a product of three matrices, $\mathbf{UxSxV^T}$. **U** is a 50 × 50 orthogonal matrix of the fraction sickled versus time at 50 time points for the images in each of the 384 wells; **S** is a 50 × 384 matrix with nonzero elements (the so-called singular values) only on the principal diagonal, which is a measure of the contribution of each component of **U** to **D**; and **V** is a 50 × 384 matrix, the columns of which are the amplitudes for each component of **U**. All but the first two or three components of the SVD represent primarily noise. As judged by the magnitude of the singular values, the complete set of 384 sickling curves on a single well plate could therefore be sufficiently well represented noise-free by just the first component of the SVD (i.e., S1 × U1 × V1). If, for a particular concentration of the test compound, $(\langle V1_{nc}\rangle - V1_{cpd})/\sigma_{nc}$, the average V1 for the negative control wells minus V1 for the test compound well divided by σ_{nc}, the SD from the average V1 for the control wells, is positive and larger than 3, it is considered antisickling. The SD of V1 is a single number and is therefore independent of time, explaining the difference in the time dependence between the SDs in the raw sickling curves and the sickling curves resulting from the SVD. Because sickling curves for the

Table 2. Average compositions and MCHCs for blood samples of various sickle syndromes in Fig. 6

Condition	%HbS	%HbF	%HbA2	%HbA	%HbC	%HbA(T87Q)	MCHC (g/dL)
HbSS off HU	88.1 ± 6.7	7.9 ± 7.2	3.7 ± 0.8	0	0	0	35.0 ± 1.5
HbSS on HU	80.0 ± 8.1	16.3 ± 8.2	4.7 ± 9.9	0	0	0	35.1 ± 1.4
HbSC disease	48.4 ± 1.6	2.1 ± 4.0	4.0 ± 0.3	0	45.6 ± 2.4	0	36.1 ± 1.0
HbS/HPFH	60.2	38.0	1.8	0	0	0	35.8
HBSS/HbA(T87Q)	44.8 ± 10.2	2.9 ± 3.5	2.8 ± 0.5	0	0	44.5 ± 5.2	33.8 ± 0.61
Sickle trait (AS)	37.5 ± 3.6	0.3 ± 0.6	3.3 ± 0.2	59.1 ± 3.1	0	0	33.8 ± 0.35

negative controls vary with row number, presumably because of small differences in the rate of deoxygenation Hb inside the red cells sitting at the bottom of the well, the values of V1 for the row of the test compound plus the V1s for negative controls from 2 adjacent rows were used to obtain $\langle V1_{nc} \rangle$, apart from rows 2 and 15. In this case the V1s from only 1 adjacent row were used to calculate $\langle V1_{nc} \rangle$. To improve the accuracy of $\langle V1_{nc} \rangle$, the V1s for sickling curves from an additional 12 (or 8) wells that contain 1, 3, and 10 nM of the test compound were also used as negative controls, since no antisickling was observed for any of the compounds at these concentrations (Table 1).

Even though the concentration of HbS in the hypo-osmolar buffer of the positive controls is too low for any polymerization to occur, the image analysis algorithm invariably counted a small fraction as sickled because of changes over the duration of the assay (hours). Since such changes could also occur for cells incubated with test compounds, the percentage of inhibition of sickling in the wells containing test compounds was defined as

$$\text{percent inhibition} = 100 \times \left[1 - \frac{V1_{cpd} - \langle V1_{pc} \rangle}{\langle V1_{nc} \rangle - \langle V1_{pc} \rangle} \right]. \quad \textbf{[1]}$$

Fitting Dose-Response Data with Smooth Curve. The model used to provide a least-squares description of the dose-response data is very similar to the log-logistic model proposed in Eq. 2 of the paper by Ritz et al. (62):

$$f(\log_{10} c) = 1 - \frac{A}{1 + \exp\left(B(\log_{10} c - \log_{10} IC50) \right)}, \quad \textbf{[2]}$$

where c is the compound concentration. The 3 adjustable parameters are A, B, and $\log_{10} IC_{50}$, the concentration in micromolar at 50% inhibition. An assumption in using Eq. 2 is that inhibition is complete, $f(\log c) = 1$ at infinite compound concentration. Constraints were applied to keep the value of the function close to 0 at the lowest compound concentrations and to ensure that the fitted curves have a sigmoid shape. The sum of squares (ssq) was minimized with the constraint terms $f1$ and $f2$ determined empirically.

$$ssq = \sum_i \left((\log_{10} c)_i^{fit} - (\log_{10} c)_i \right)^2 + f1 + f2$$

$$f1 = \exp(15 + B) + \exp(-0.5 - B)$$

$$f2 = \exp(0.5 - A) + \exp(A - 1.5) - 2\exp(-0.5).$$

The term $f1$ constrains the curve to have a sigmoid shape with the adjustable parameter, B. The term $f2$ is an additional constraint with the adjustable parameter of A. In the log-logistic model, A is the difference between the upper and lower asymptotes of the response, which in the SVD analysis is the difference between $\langle V1_{nc} \rangle$ and $\langle V1_{pc} \rangle$. At concentrations too low to be inhibitory, $(S1 \times U1 \times V1)_{cpd}$ can be larger than $\langle (S1 \times U1 \times V1)_{nc} \rangle$, which produces negative deviations from 0. After fitting, differences between the fitted and experimental points (residuals) were fit to a Gaussian distribution. If a residual was >3 SDs from the mean, then the relevant experimental point was removed as an outlier. The data were then refit with the outliers removed.

Data, Materials, and Software Availability. All of the study data are included in the article and/or *SI Appendix*.

Author affiliations: ᵃLaboratory of Chemical Physics, National Institute of Diabetes and Digestive and Kidney Diseases, Bethesda, MD 20892; ᵇOffice of the Clinical Director, National Institute of Diabetes and Kidney Diseases, Bethesda, MD 20892; ᶜCellular and Molecular Therapeutics Branch, National Heart, Lung, and Blood Institute, National Institutes of Health, Bethesda, MD, 20892; ᵈSickle Cell Branch, National Heart, Lung, and Blood Institute, National Institutes of Health, Bethesda, MD, 20892; and ᵉDepartment of Medicinal Chemistry, Calibr at Scripps Research, La Jolla, CA 92037

Author contributions: W.A.E. conceived the project, directed the research and wrote the manuscript; A.K.C. provided the compound library and annotations; B.M. measured sickling curves for sickle trait samples; Q.L. measured sickling curves for SCD samples; T.C. analyzed sickling data; J.H. introduced application of singular value decomposition; E.R.H. developed the image analysis algorithm for counting sickled cells; E.B. D. organized all data and results of image analysis; M.H., J.F.T., A.C., D.S., and S.L.T. recruited blood donors; E.B.D., S.L.T., and J.F.T edited the manuscript.

1. L. Pauling, H. A. Itano, S. J. Singer, I. C. Wells, Sickle cell anemia a molecular disease. *Science* **110**, 543–548 (1949).
2. W. A. Eaton, Linus Pauling and sickle cell disease. *Biophys. Chem.* **100**, 109–116 (2003).
3. V. M. Ingram, Gene mutations in human haemoglobin: The chemical difference between normal and sickle cell haemoglobin. *Nature* **180**, 326–328 (1957).
4. M. F. Perutz, H. Lehmann, Molecular pathology of human haemoglobin. *Nature* **219**, 902–909 (1968).
5. H. F. Bunn, B. G. Forget, *Hemoglobin: Molecular, Genetic, and Clinical Aspects* (Saunders, New York, 1986), pp. 610.
6. H. F. Bunn, Pathogenesis and treatment of sickle cell disease. *N. Engl. J. Med.* **337**, 762–769 (1997).
7. W. A. Eaton, H. F. Bunn, Treating sickle cell disease by targeting HbS polymerization. *Blood* **129**, 2719–2726 (2017).
8. A. Rankine-Mullings et al., Hydroxycarbamide treatment reduces transcranial Doppler velocity in the absence of transfusion support in children with sickle cell anaemia, elevated transcranial Doppler velocity, and cerebral vasculopathy: The EXTEND trial. *Br. J. Haematol.* **195**, 612–620 (2021).
9. E. R. Henry et al., Treatment of sickle cell disease by increasing oxygen affinity of hemoglobin. *Blood* **138**, 1172–1181 (2021).
10. C. T. Quinn, R. E. Ware, Increased oxygen affinity: To have and to hold. *Blood* **138**, 1094–1095 (2021).
11. Y. Niihara, W. R. Smith, C. W. Stark, A Phase 3 trial of l-glutamine in sickle cell disease. *N. Engl. J. Med.* **379**, 1880 (2018).
12. M. H. Steinberg et al.; Investigators of the Multicenter Study of Hydroxyurea in Sickle Cell Anemia and MSH Patients' Follow-Up, The risks and benefits of long-term use of hydroxyurea in sickle cell anemia: A 17.5 year follow-up. *Am. J. Hematol.* **85**, 403–408 (2010).
13. N. Vasavda et al., The presence of alpha-thalassaemia trait blunts the response to hydroxycarbamide in patients with sickle cell disease. *Br. J. Haematol.* **143**, 589–592 (2008).
14. W. A. Eaton, J. Hofrichter, The biophysics of sickle cell hydroxyurea therapy. *Science* **268**, 1142–1143 (1995).
15. P. T. McGann, R. E. Ware, Hydroxyurea therapy for sickle cell anemia. *Expert Opin. Drug Saf.* **14**, 1749–1758 (2015).
16. J. F. Tisdale, S. L. Thein, W. A. Eaton, Treating sickle cell anemia. *Science* **367**, 1198–1199 (2020).
17. F. B. Piel, The present and future global burden of the inherited disorders of hemoglobin. *Hemat.-Onco.Clin. North America* **30**, 327–341 (2016).
18. E. B. Dunkelberger, B. Metaferia, T. Cellmer, E. R. Henry, Theoretical simulation of red cell sickling upon deoxygenation based on the physical chemistry of sickle hemoglobin fiber formation. *J. Phys. Chem. B* **122**, 11579–11590 (2018).
19. J. Janes et al., The ReFRAME library as a comprehensive drug repurposing library and its application to the treatment of cryptosporidiosis. *Proc. Natl. Acad. Sci. U.S.A.* **115**, 10750–10755 (2018).
20. E. L. Berg, The future of phenotypic drug discovery. *Cell Chem. Biol.* **28**, 424–430 (2021).
21. Q. Li et al., Kinetic assay shows that increasing red cell volume could be a treatment for sickle cell disease. *Proc. Natl. Acad. Sci. U.S.A.* **114**, E689–E696 (2017).
22. H. S. Zarkowsky, R. M. Hochmuth, Sickling times of individual erythrocytes at zero Po2. *J. Clin. Invest.* **56**, 1023–1034 (1975).
23. M. Coletta, J. Hofrichter, F. A. Ferrone, W. A. Eaton, Kinetics of sickle haemoglobin polymerization in single red cells. *Nature* **300**, 194–197 (1982).
24. F. A. Ferrone, J. Hofrichter, W. A. Eaton, Kinetics of sickle hemoglobin polymerization. II. A double nucleation mechanism. *J. Mol. Biol.* **183**, 611–631 (1985).
25. W. A. Eaton, J. Hofrichter, Sickle cell hemoglobin polymerization. *Adv. Protein Chem.* **40**, 63–279 (1990).
26. G. W. Christoph, J. Hofrichter, W. A. Eaton, Understanding the shape of sickled red cells. *Biophys. J.* **88**, 1371–1376 (2005).
27. C. Brugnara, H. F. Bunn, D. C. Tosteson, Regulation of erythrocyte cation and water content in sickle cell anemia. *Science* **232**, 388–390 (1986).
28. W. N. Poillon, B. C. Kim, 2,3-Diphosphoglycerate and intracelluar pH as determinants of the physiological solubility of deoxyhemoglobin S. *Blood* **76**, 1028–1036 (1990).
29. W. N. Poillon, B. C. Kim, R. J. Labotka, C. U. Hicks, J. A. Kark, Antisickling effects of 2,3-diphosphoglycerate depletion. *Blood* **85**, 3289–3296 (1995).
30. J. Hofrichter, P. D. Ross, W. A. Eaton, Supersaturation in sickle cell hemoglobin solutions. *Proc. Natl. Acad. Sci. U.S.A.* **73**, 3035–3039 (1976).
31. M. A. Goldberg, M. A. Husson, H. F. Bunn, Participation of hemoglobins A and F in polymerization of sickle hemoglobin. *J. Biol. Chem.* **252**, 3414–3421 (1977).
32. R. W. Briehl, Gelation of sickle cell hemoglobin. IV. Phase transitions in hemoglobin S gels: Separate measures of aggregation and solution–gel equilibrium. *J. Mol. Biol.* **123**, 521–538 (1978).

33. W. A. Eaton, J. Hofrichter, P. D. Ross, Editorial. Delay time of gelation: A possible determinant of clinical severity in sickle cell disease. *Blood* **47**, 621–627 (1976).

34. H. R. Sunshine, J. Hofrichter, F. A. Ferrone, W. A. Eaton, Oxygen binding by sickle cell hemoglobin polymers. *J. Mol. Biol.* **158**, 251–273 (1982).

35. E. R. Henry *et al.*, MWC allosteric model explains unusual hemoglobin-oxygen binding curves from sickle cell drug binding. *Biophys. J.* **120**, 2543–2551 (2021).

36. S. Charache *et al.*; Investigators of the Multicenter Study of Hydroxyurea in Sickle Cell Anemia, Effect of hydroxyurea on the frequency of painful crises in sickle cell anemia. *N. Engl. J. Med.* **332**, 1317–1322 (1995).

37. K. R. Bridges *et al.*, A multiparameter analysis of sickle erythrocytes in patients undergoing hydroxyurea therapy. *Blood* **88**, 4701–4710 (1996).

38. D. E. Bauer, S. C. Kamran, S. H. Orkin, Reawakening fetal hemoglobin: Prospects for new therapies for the β-globin disorders. *Blood* **120**, 2945–2953 (2012).

39. C. T. Quinn *et al.*, Early initiation of hydroxyurea (hydroxycarbamide) using individualised, pharmacokinetics-guided dosing can produce sustained and nearly pancellular expression of fetal haemoglobin in children with sickle cell anaemia. *Br. J. Haematol.* **194**, 617–625 (2021).

40. R. E. Ware, S. D. Dertinger, Absence of hydroxyurea-induced mutational effects supports higher utilisation for the treatment of sickle cell anaemia. *Br. J. Haematol.* **194**, 252–266 (2021).

41. J. Kanter *et al.*, Biologic and clinical efficacy of lentiglobin for sickle cell disease. *N. Engl. J. Med.* **386**, 617–628 (2022).

42. E. R. Henry, J. Hofrichter, Singular value decomposition: Application to analysis of experimental data. *Methods Enzymol.* **210**, 129–192 (1992).

43. R. Pawliuk *et al.*, Correction of sickle cell disease in transgenic mouse models by gene therapy. *Science* **294**, 2368–2371 (2001).

44. A. A. Abraham, J. F. Tisdale, Gene therapy for sickle cell disease: Moving from the bench to the bedside. *Blood* **138**, 932–941 (2021).

45. R. L. Nagel *et al.*, Structural bases of the inhibitory effects of hemoglobin F and hemoglobin A2 on the polymerization of hemoglobin S. *Proc. Natl. Acad. Sci. U.S.A.* **76**, 670–672 (1979).

46. H. F. Bunn *et al.*, Molecular and cellular pathogenesis of hemoglobin SC disease. *Proc. Natl. Acad. Sci. U.S.A.* **79**, 7527–7531 (1982).

47. R. L. Nagel, M. E. Fabry, M. H. Steinberg, The paradox of hemoglobin SC disease. *Blood Rev.* **17**, 167–178 (2003).

48. E. R. Henry *et al.*, Allosteric control of hemoglobin S fiber formation by oxygen and its relation to the pathophysiology of sickle cell disease. *Proc. Natl. Acad. Sci. U.S.A.* **117**, 15018–15027 (2020).

49. J. Hofrichter, P. D. Ross, W. A. Eaton, Kinetics and mechanism of deoxyhemoglobin S gelation: A new approach to understanding sickle cell disease. *Proc. Natl. Acad. Sci. U.S.A.* **71**, 4864–4868 (1974).

50. W. A. Eaton, J. Hofrichter, Hemoglobin S gelation and sickle cell disease. *Blood* **70**, 1245–1266 (1987).

51. W. A. Eaton, Hemoglobin S polymerization and sickle cell disease: A retrospective on the occasion of the 70th anniversary of Pauling's *Science* paper. *Am. J. Hematol.* **95**, 205–211 (2020).

52. W. A. Eaton, Impact of hemoglobin biophysical studies on molecular pathogenesis and drug therapy for sickle cell disease. *Mol. Aspects Med.* **84**, 100971 (2022).

53. A. C. Geisness *et al.*, Ionophore-mediated swelling of erythrocytes as a therapeutic mechanism in sickle cell disease. *Haematologica* **107**, 1438–1447 (2022).

54. O. Castro, W. N. Poillon, H. Finke, E. Massac, B. C. Kim, Improvement of sickle cell anemia by iron-limited erythropoiesis. *Am. J. Hematol.* **47**, 74–81 (1994).

55. N. Vunnam *et al.*, Fluorescence lifetime measurement of prefibrillar sickle hemoglobin oligomers as a platform for drug discovery in sickle cell disease. *Biomacromolecules* **23**, 3822–3830 (2022).

56. J. Z. Xu *et al.*, A Phase 1 dose scalation study of the pyruvate kinase activator mitapivat (AG-348) in sickle cell disease. *Blood*. https://doi.org/10.1182/blood.2022015403.

57. T. Cellmer, F. A. Ferrone, W. A. Eaton, Universality of supersaturation in protein-fiber formation. *Nat. Struct. Mol. Biol.* **23**, 459–461 (2016).

58. A. Mozzarelli, J. Hofrichter, W. A. Eaton, Delay time of hemoglobin S polymerization prevents most cells from sickling in vivo. *Science* **237**, 500–506 (1987).

59. E. Evans, Y. C. Fung, Improved measurements of erythrocyte geometry. *Microvasc. Res.* **4**, 335–347 (1972).

60. G. Di Caprio, C. Stokes, J. M. Higgins, E. Schonbrun, Single-cell measurement of red blood cell oxygen affinity. *Proc. Natl. Acad. Sci. U.S.A.* **112**, 9984–9989 (2015).

61. G. Di Caprio *et al.*, High-throughput assessment of hemoglobin polymer in single red blood cells from sickle cell patients under controlled oxygen tension. *Proc. Natl. Acad. Sci. U.S.A.* **116**, 25236–25242 (2019).

62. C. Ritz, F. Baty, J. C. Streibig, D. Gerhard, Dose-response analysis using R. *PLoS One* **10**, e0146021 (2015).